Contents list available at **IJND**

# International Journal of Nano Dimension

Journal homepage: *www.IJND.ir*

# Simulation of nanodroplet impact on a solid surface

## ABSTRACT

**S. Asadi**[*]

*Department of Mechanical Engineering, Payame Noor University,* Tehran, *Iran.*

A novel computational fluid dynamics and molecular kinetic theory (CFD-MK) method was developed to simulate the impingement of a nanodroplet onto a solid surface. A numerical solution of the Navier–Stokes equation using a volume-of-fluid (VOF) technique was used to model nanodroplet deformation. Dynamic contact angle during droplet impact was obtained by molecular kinetic theory. This dynamic contact angle was then implemented in the numerical model used to simulate the process. The spreading behavior was analyzed for the wettable, partially wettable and nonwettable surfaces. The consistency between the two results was good both qualitatively and quantitatively.

**Keywords:** *Nanodroplet impact; Free surface flows; Molecular kinetic theory; Numerical simulation; Computational fluid dynamics(CFD).*

## INTRODUCTION

Spreading of nanodroplets on solid surfaces is important in a wide variety of applications, including ink jet printing, DNA synthesis, etc [1,2]. A new approach in nano-manufacturing and nano-fabricating is the ink jet printing technique. InkJet printing is one of the most attractive techniques for fabricating nano-devices [3-6]. In the new type of inkjet printers, precise print of dots in the range of few hundreds of nanometer can be developed, which could be used to synthesize complex nanoscale structures out of various materials [5, 6]. Since the operational costs of inkjet printing equipment is high, it is more economical to optimize operating parameters using computational models. Development of theoretically computational models, which can predict nanodroplet deposition, can potentially reduce the cost of the development of new process considerably. Ideally, these models will allow us to tailor deposition properties to meet the requirements of individual applications, without having anything to do with extensive experimentation. The models will also allow us to improve and optimize the design of existing systems.

* Corresponding author:
Saeid Asadi
Department of Mechanical Engineering, Payame Noor University, *PO BOX 19395-3697,* Tehran, Iran
Tel +98 2126120017
Fax +98 2126120017
*Email  s_asadi@pnu.ac.ir*

Computational fluid dynamics (CFD), based on the continuum Euler and Navier– Stokes equations for inviscid and viscous flow modelling, respectively, is the most common tool to simulate the microdroplet impact on solid surface [7- 9]. Luckily, above 10 molecular diameters, systems can very often be described with continuum theory, which statistically averages the single interactions [10]. Deviations from the predictions of classical continuum theory have been observed for a liquid confined in a space smaller than 10 molecular diameters, especially in the microscopic layer in the vicinity of the moving contact line [2]. Molecular dynamics (MD) simulations are, therefore, appropriate for such systems. Thus, the alternative is to use the molecular dynamics (MD) method [1], an atomistic description that considers atoms as point masses whose motion is governed by the Newton's equation of motion in conjunction with a model for the interatomic forces. MD is computer intensive and even by using the most powerful massively parallel computers, this approach is presently only applicable to small systems [11].

In many applications where the phenomena of interest range from macro to nanoscale, the continuum-based equations (Euler/Navier–Stokes) will still be valid in large parts of the computational domain but continuum approaches fail to describe the nanofluidic flows where the continuum equations have essential singularities, as in the moving contact-line problem [12,13].

For characterizing the spreading behavior of a nanodroplet, it is important to report the contact angles around the contact line. The dynamic effects on contact angle due to the contact-line motion are important. The development of new methods will enable the CFD simulation of larger domains than those presently computed using MD and is of interest in a broad range of flows, which are subject to an interplay between the macroscopic dynamics of the bulk flow and microscopic and molecular kinetic (MK) at molecular scale around the fluid–solid contact line. A literature survey carried out by the authors indicated lack of published data on the nanodroplet impact simulation by computational fluid dynamics and molecular kinetic theory (CFD-MK).

There exists a considerable literature describing CFD models of microdroplet impact on a solid surface [7, 9,14].

Sedighi et al. [1] studied the process of a single nanodroplet impact onto a surface with a molecular dynamics simulation (MD) using the interactions between molecules were represented by the Lennard-Jones (LJ) potential. They found that the dynamic contact angle and spreading diameter, as well as the advancing and receding time periods, exhibit strong dependence on droplet size.

In this paper, a novel simulation by computational fluid dynamics and molecular kinetic theory (CFD-MK) is presented. The molecular contact angle couples with the continuum model by performing molecular dynamics contact angle around at the contact line of the macroscopic CFD solver, which is engaged to advance the simulation. The numerical model is validated by qualitatively and quantitatively comparing with the MD method of Sedighi et al. [1].

## EXPERIMENTAL

### Governing Equations

A schematic of a droplet impact on a surface is shown in Figure 1. The mathematical description of the problem is formulated subject to these assumptions:

(i) the droplet is spherical prior to impact, (ii) ) the system (above 10 molecular diameters) can be described with continuum theory, which statistically averages the single interactions [10], (iii) the liquid is incompressible and Newtonian, (iv) the liquid density, viscosity and surface tension are constant, (v) the flow during the impact is laminar [8, 9, 15], (vi) a single velocity characterizes fluid motion prior to the impact (which precludes considering an internal circulation of the fluid within the droplet prior to the impact), and (vii) the influence of the surrounding gas on the liquid during the impact is negligible (which implies that viscous stresses at the free surface are assumed to be zero).
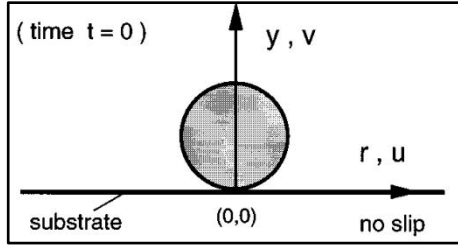
**Fig. 1.** A schematic of a droplet impact on a surface.

The equations of conservation of mass and momentum in the liquid may then be written as [8, 9]:

$$\nabla \cdot \vec{V} = 0 \qquad (1)$$

$$\frac{\partial \vec{V}}{\partial t} + \nabla \cdot (\vec{V}\vec{V}) = -\frac{1}{\rho}\nabla P + \frac{1}{\rho}\nabla \cdot \tilde{\tau} + \vec{g} + \frac{1}{\rho}\vec{F}_b \qquad (2)$$

where $\vec{V}$ represents the velocity vector, $P$ the pressure, $\rho$ the liquid density, $\tilde{\tau}$ the shear stress tensor, $\vec{g}$ the gravitational acceleration, and $\vec{F}_b$ any body forces (per unit volume) acting on the fluid.

The flow equations have been written in an Eulerian frame of reference, and thus a solution of these equations must be coupled with some methodology for following the deforming liquid-gas interface. The VOF technique is applied to track the time evolution of the liquid free surface. A color function, *f*, is introduced to represent the volume fraction of liquid in a computational cell. If the control volume is filled with liquid alone, the color function will be unity. When only air exists in the control volume, *f* takes on a value of zero. When both liquid and gas are present, the color function value lies between zero and one. The advection of function *f* is governed by [8, 9]:

$$\frac{\partial f}{\partial t} + (\vec{V} \cdot \nabla)f = 0 \qquad (3)$$

The volume force, $\vec{F}_b$, appearing in Eq. (2), consists of the gravitational force and the surface tension force which is given as [16]

$$\vec{F}_{ST}(x) = \gamma \int_s k(\vec{y})\hat{n}(\vec{y})\,\delta(\vec{x} - \vec{y})\,dS \qquad (4)$$

by means of the CSF model. In this equation, $\hat{n}$ represents a unit vector normal to the interface directed into the liquid, $\gamma$ represents the liquid-gas surface tension and *k* the total curvature of the interface, $\delta$ is the Dirac delta function, and $\vec{x}$ and $\vec{y}$ are position vectors. The integration is performed over some area of free surface *S*. *k* and $\hat{n}$ are geometric characteristics of the surface, and may be written in terms of *f*:

$$k = -\nabla . \hat{n} \quad , \quad \hat{n} = \frac{\nabla f}{\left|\nabla f\right|} \qquad (5)$$

Expressed as a body force, surface tension is then incorporated into Eq. (2) via the term $\vec{F}_b$. To reduce the size of the computational domain, symmetric boundaries are applied when possible. Along a symmetric boundary, fluid velocity obeys slip and no penetration conditions. Boundary conditions are also imposed at the liquid free surface, denoted by subscript *s*. The boundary condition on velocity is the zero shear stress condition:

$$\tau_s = 0 \qquad (6)$$

and since the surface tension force has been included in Eq. (2), the boundary condition on pressure reduces to:

$$p_s = 0 \qquad (7)$$

A boundary condition for *f* is unnecessary since *f* is a Lagrangian invariant. Initial condition for *f* is defined by specifying a droplet diameter $D_o$. Fluid velocity within the droplet is characterized by a single impact velocity and the initial pressure within the droplet is defined by the Laplace equation:

$$\vec{V} = \vec{V}_0 \ , \quad P_0 = 4\frac{\gamma}{D_0} \qquad (8)$$

***Molecular-kinetic (M-K) theory***

The molecular-kinetic theory of wetting, as developed by Blake & Haynes [17], uses the theory of absolute reaction rates and asserts that the

essential contact line motion takes place by jumping of molecules along the solid surface from the liquid to the vapour side of the contact line. According to this theory, the macroscopic behaviour of the wetting line depends on the overall statistics of the individual molecular displacements, which occur within the three-phase zone where the fluid– fluid interface meets the solid surface. The molecular-kinetic theory postulates that the entire energy dissipation occurs at the moving contact line. The wetting line moves with velocity $V_{CL}$, and the liquid exhibits a dynamic advancing contact angle $\theta$ such that $\theta > \theta_E$, where $\theta_E$ is the equilibrium contact angle. According to this theory, the velocity of the contact line is determined by the frequency $\kappa$ and length $\lambda$ of the individual molecular displacements that occur along its length. In the simplest model, these displacements take place at the adsorption sites on the solid surface. The length of the molecular displacement $\lambda$ is influenced by the size of the liquid molecules and depends strongly on the spacing of the successive adsorption sites on the target surface. For the liquid molecules moving forward, the frequency of molecular displacement is $\kappa+$, and for those moving backwards, the frequency is $\kappa-$. The contact line velocity is then given by $V_{CL} = (\kappa+ - \kappa-)\lambda = \kappa\lambda$, where $\kappa$ is the net frequency of molecular displacement (jump frequency). For the contact line to move, work must be done to overcome the energy barriers to molecular displacement in the preferred direction. This work is done by the surface tension force, which is $\sigma(\cos \theta_E - \cos \theta)$, as expressed per unit length of the contact line. The work done by this force is entirely within the contact point zone and any dissipation outside of this zone neglected in the model. Combining these ideas and using Frenkel–Eyring activated rate theory of transport in liquids, the following relationship between $\theta$ and $V_{CL}$ was obtained by Megaridis [18]:

$$V_{CL} = \frac{2\kappa_S h\lambda}{\mu\nu} \sinh\left[\frac{\gamma}{2nkT}(\cos\theta_e - \cos\theta)\right] \quad (9)$$

Where $k$, $T$ denote, respectively, Boltzmann's constant and the absolute temperature. The quantity $n$ is the number of adsorption sites per unit area on the surface and is

related to $\lambda$ by $\lambda \sim n^{-1/2}$. the solid/liquid interaction frequency $\kappa_s$ is:

$$\kappa_s = \frac{kT}{h}\exp(\frac{-\Delta G_S}{N_A kT}) \quad (10)$$

Where $-\Delta G_S$ is the contribution arising from the retarding influence of the solid surface, $N_A$ is Avogadro's number and $h$ stands for Planck's constant [18].

## NUMERICAL PROCEDURE

Figure 2 illustrates a typical mesh where velocities are specified at the centre of cell faces and pressure at each cell centre.
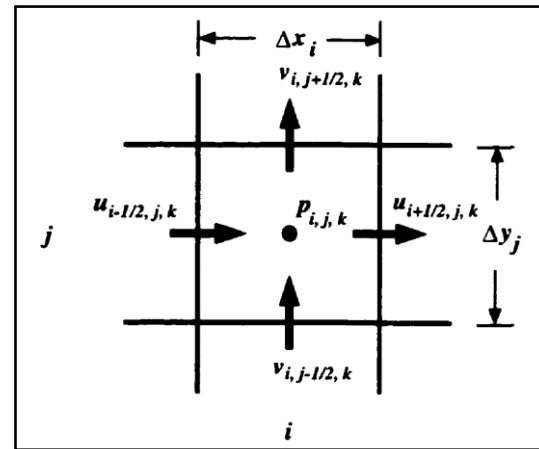


**Fig. 2.** A 2D control volume, with velocities specified at cell faces, pressure at the cell center.

Equations (1) and (2), are solved with a two-step projection method, in which a forward Euler time discretization of the momentum equation is divided into two steps:

$$\frac{\vec{V}' - \vec{V}^n}{\Delta t} = -\nabla\cdot(\vec{V}\vec{V})^n + \frac{1}{\rho}\nabla\cdot\tilde{\tau}^n + \vec{g}^n + \frac{1}{\rho}\vec{F}_b^n \quad (11)$$

$$\frac{\vec{V}^{n+1} - \vec{V}'}{\Delta t} = -\frac{1}{\rho^n}\nabla P^{n+1} \quad (12)$$

In the first step, using Eq. (11), an interim velocity $\vec{V}'$ is computed explicitly from convective, viscous, gravitational and body force

accelerations of the known field $\vec{V}^n$ for a timestep $\Delta t$. In the second step, using Eq. (12), $\vec{V}^n$ is projected onto a divergence-free velocity field. Combining Eq. (12) with Eq. (1) at the new time level *(n+1)* yields a Poisson equation for pressure:

$$\nabla \cdot (\frac{1}{\rho^n}\nabla P^{n+1}) = \frac{1}{\Delta t}\nabla \cdot \vec{V}' \tag{13}$$

The RHS of Eq. (11) is discretized according to the conventions typical of the finite volume method**.** Integrating Eq. (11) over a control volume $\Omega_{i,j}$ yields:

$$\frac{1}{\Delta t}\int_{\Omega_{i,j}}(\vec{V}'-\vec{V}^n)d\Omega = -\int_{\Omega_{i,j}}\nabla \cdot (\vec{V}\vec{V})^n d\Omega + \frac{1}{\rho}\int_{\Omega_{i,j}}\nabla \cdot \tilde{\tau}^n d\Omega + \int_{\Omega_{i,j}}\vec{g}^n d\Omega + \frac{1}{\rho}\int_{\Omega_{i,j}}\vec{F}_b^n d\Omega \tag{14}$$

Applying Gauss' theorem to convert the first two volume integrals on the RHS to integrals over the control volume surface $S_{i,j}$ and assuming that the other integrands are constant throughout $\Omega_{i,j}$, Eq. (14) becomes:

$$\frac{\vec{V}'-\vec{V}^n}{\Delta t} = -\frac{1}{\Omega_{i,j}}\int_{S_{i,j}}\vec{V}^n(\vec{V}^n \cdot \hat{n}_S)dS + \frac{1}{\rho\Omega_{i,j}}\int_{S_{i,j}}(\tilde{\tau}^n \cdot \hat{n}_S)dS + \vec{g}^n + \frac{1}{\rho}\vec{F}_b^n \tag{15}$$

where $\hat{n}_S$ is the unit outward normal to $S_{i,j}$.

Following algorithm advances the solution by one timestep. Given velocity, pressure, and volume fraction fields at the time level *n*:

1. evaluate $\vec{V}'$ using Eq. (11)
2. solve Eq. (13) implicitly for $P^{n+1}$, incorporating boundary conditions on $P$
3. evaluate $\vec{V}^{n+1}$ using Eq. (12)
4. apply boundary conditions on $\vec{V}^{n+1}$
5. evalute $\theta$ from molecular-kinetic theory by using Eq. (9)
6. evaluate $\vec{n}_{i,j}$ and $\hat{n}$ from $\theta$
7. evaluate a new fluid volume distribution $f^{n+1}$ using Eq. (3) and obtain the new shape of liquid-gas free surface using Youngs' algorithm [19]
8. reapply boundary conditions on $\vec{V}^{n+1}$

Repetition of these steps allowed advancing the solution through an arbitrary time interval. The computational domain encompassed the initial droplet and sufficient volume for the droplet spreading during the impingement. The mesh size was determined on the basis of a mesh refinement study in which the grid spacing was progressively decreased until further reductions made no significant changes in the predicted shape during the impact. The droplet was discretized using a computational mesh, with a uniform grid spacing equal to 1/30 of the droplet radius. Numerical computations were performed on a Pentium 4 computer. Typical CPU times ranged from four to five hours.

## RESULTS AND DISCUSSION

In order to validate the simulation model, we compared our simulation results with MD simulations of Sedeghi et al. [1] for the impact of a 6 nm argon nanodroplet on flat surfaces with different wetting characteristics. The MD photographs are taken from a study conducted by sedighi et al. [1], who have described the MD simulation in detail.

They examined the spreading behavior of nano-sized liquid argon droplets on solid surfaces using MD simulations. They presented their results for three cases with different values for the three different surfaces, wettable ($\theta_0 < 40$), partially wettable ($40 < \theta_0 < 140$) and non-wettable ($\theta_0 > 140$).

Figure 3 compares images calculated using our numerical CFD-MK model with MD model given by Sedeghi et al. [1] for wettable surface case where the diameter ($D_0$) of the argon nanodroplet was 6 nm and the initial velocity($V_0$) $1.25ms^{-1}$.

In addition Figure 4 and 5 compare images for partially wettable and non-wettable surfaces where the diameter ($D_0$) of the argon nanodroplet was 6 nm and the initial velocity ($V_0$) $1.25ms^{-1}$.
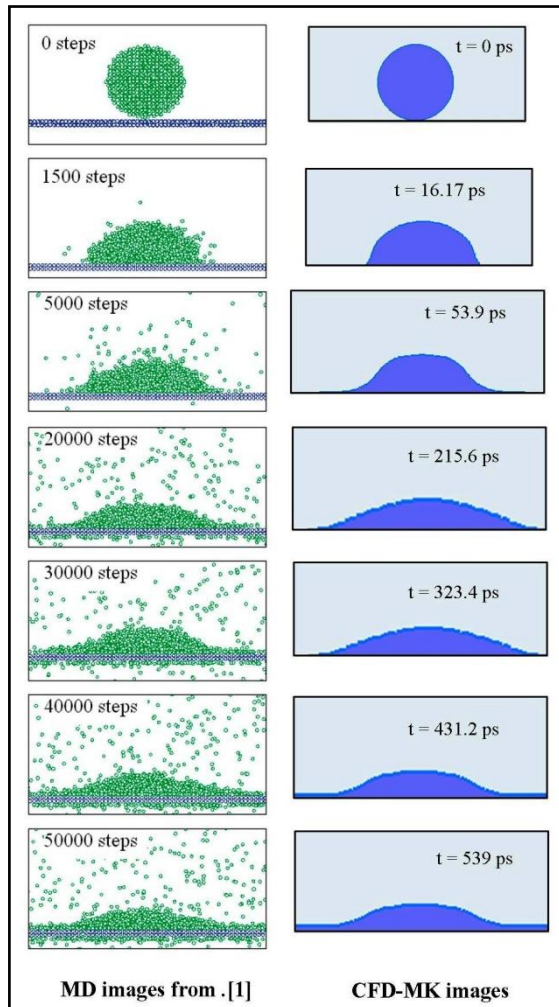
**Fig. 3.** MD images [1]. and CFD-MK images of a 6 nm nanodroplet impacting with a velocity of 1.25 m/s on flate wettable surface.



**Fig. 4.** MD images [1]. and CFD-MK images of a 6 nm nanodroplet impacting with a velocity of 1.25 m/s on flate partially wettable surface.

As observed from Figures 3-5, there are a good qualitative agreement between numerical CFD-MK model and MD simulation images. The spreading of argon nanodroplet seen in images is well predicted by the numerical CFD-MK model. The time of each image ($t$), measured from the instant of first contact with the surface, is also indicated in the figures.

To present a quantitative comparison between the results of the model with those of the experiments, the measured data reported by Sedighi et al. [1] are used. Dividing maximum lateral spread diameter by the initial nanodroplet diameter results in the nondimensional maximum lateral spread ratio denoted by $D_m/D_o$. The $D_m/D_o$ evolution was investigated in Sedighi et al. [1]
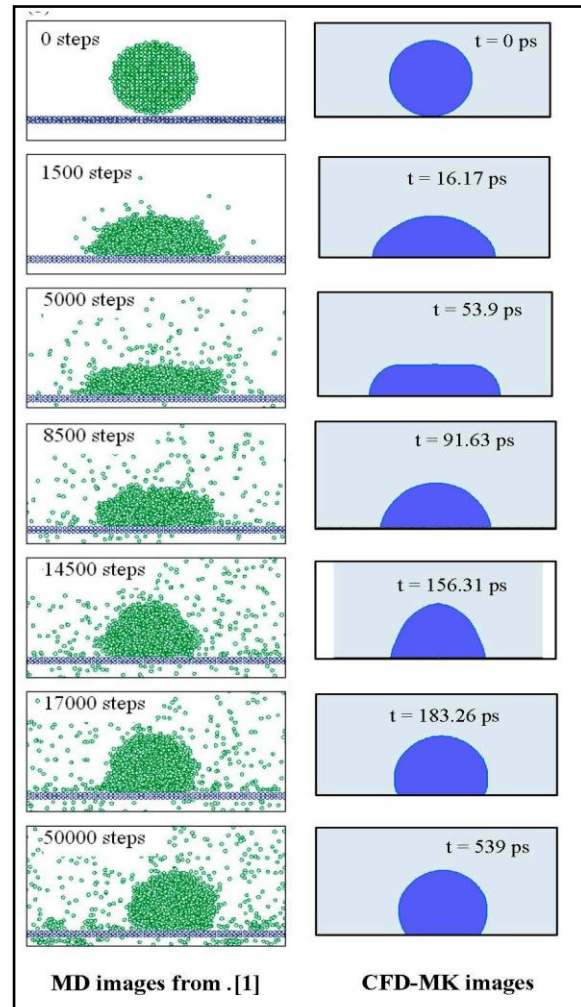
simulations by analyzing the images taken from the side. They measured the nondimensional maximum lateral spread ratio versus time for all of their simulation conditions. The results of their MD simulations are shown in Figures 6-8 where the measured variation of $D_m/D_o$ versus $t$ is plotted along with the our CFD-MK model predictions for the same conditions. The droplet diameter and impact velocity was held constant. The surface wetting characteristics, however, was changed. The value of $\theta_0$ was 20°, 74° and 135°, respectively. A good quantitative agreement between the hybrid model predictions with those of the MD simulation validates the model and its underlying assumptions.
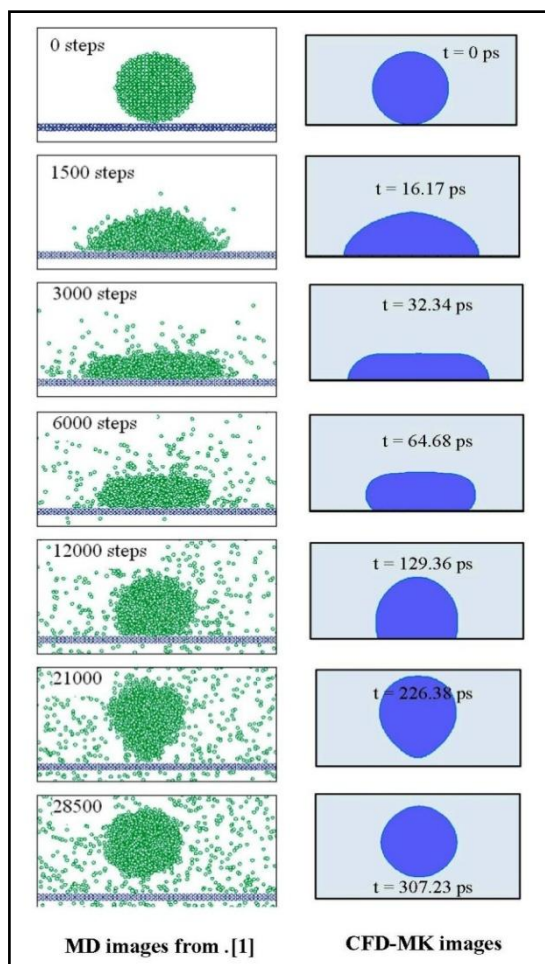
**Fig. 5.** MD images [1] and CFD-MK images of a 6 nm nanodroplet impacting with a velocity of 1.25 m/s on flate non-wettable surface.
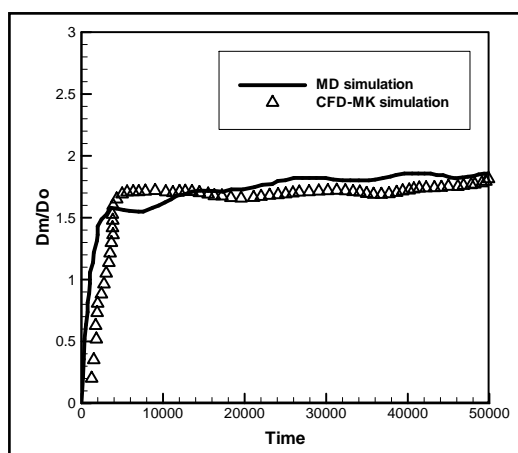


**Fig. 6.** A comparison between CFD-MK simulation and MD simulation [1] results for the evolution of nondimensional maximum lateral spread ratio of 6 nm diameter nanodroplet impacting on wettable surface. for a case with $V_0 = 1.25 \text{ms}^{-1}$.
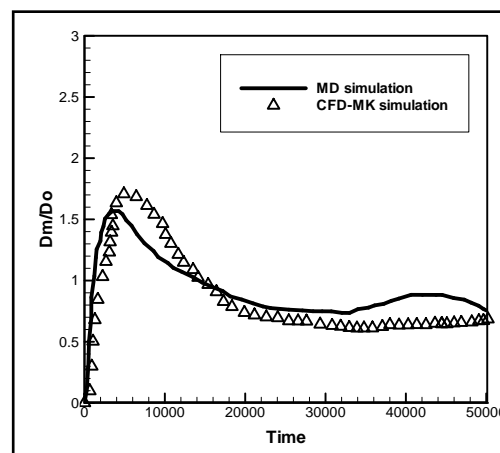


**Fig. 7.** A comparison between CFD-MK simulation and MD simulation [1] results for the evolution of nondimensional maximum lateral spread ratio of 6 nm diameter nanodroplet impacting on partially wettable surface. for a case with $V_0 = 1.25 \text{ms}^{-1}$.
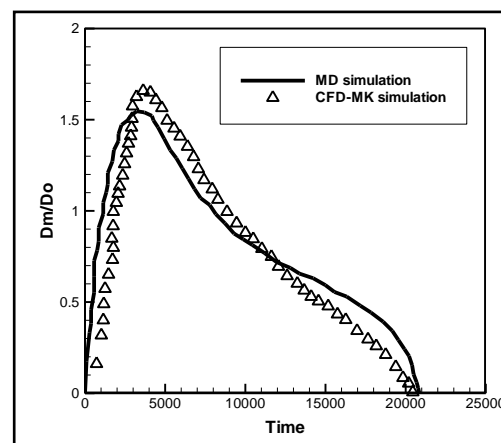


**Fig. 8.** A comparison between CFD-MK simulation and MD simulation [1] results for the evolution of nondimensional maximum lateral spread ratio of 6 nm diameter nanodroplet impacting on non-wettable surface. for a case with $V_0 = 1.25 \text{ms}^{-1}$.

## CONCLUSION

We have developed a CFD-MK (computational fluid dynamics and molecular kinetic theory) model of free surface fluid flow and applied it to simulating the impact of a nanodroplet onto a flat surface. The volume-of-fluid (VOF) technique is used to track the free-surface of the liquid. Dynamic contact angles are applied as a boundary condition at the liquid – solid contact lines and evaluated by molecular kinetic theory equation. To validate the CFD-MK model we simulated impact of argon nanodroplets onto

wettable, partial wettable and nonwettable surfaces. The consistency between the two results was good both qualitatively and quantitatively.

## ACKNOWLEDGEMENTS

## REFERENCES

[1] Sedighi N., Murad S., Aggarwal S.K., (2010). Molecular dynamics simulations of nanodroplet spreading on solid surfaces, effect of droplet size. *Fluid Dynamics Researchs* 42:1-23.

[2] Sedighi N., (2010). Investigation of spreading characteristics of nano-droplet on solid substrate using MD simulation. *PhD Thesis*, University of Illinois at Chicago.

[3] Smith P.J., Shin D.Y., Stringer I.E., Derby B., (2006). Direct ink-jet printing and low temperature conversion of conductive silver patterns. *Journal of materials science,* 41:4153-4158.

[4] Cooley P., Wallace D., Antohe B., (2001). Applications of ink-jet printing technology to BioMEMS and microfluidic systems. *Proceedings, SPIE Conference on Microfluidics and BioMEMS*, San Francisco, CA, USA.

[5] Choi C., (2003). Ink-Jet printing creates tubes of living tissue. *Newscientist*, Jan. 22.

[6] Bidoki S.M., Lewis D.M., Clark M., Vakorov A., Millner P.A., McGorman D., (2007). Ink-jet fabrication of electronic components. *Journal of Micromechanics and Microengineering*, 17:967-974.

[7] Asadi S., Passandideh-Fard M., Moghiman M., (2008). Numerical and analytical model of the inclined impact of a droplet on a solid surface in a thermal spray coating process. *Iranian Journal of Surface and Engineering*, 4:1-14.

[8] Asadi S., Passandideh-Fard M., (2009). A Computational Study On Droplet Impingement Onto A Thin Liquid Film. *The Arabian Journal for Science and Engineering*, 34(2B):505-517.

[9] Pasandideh-Fard M., Chandra S., Mostaghimi J., (2002). A three-dimensional model of droplet impact and solidification. *International Journal of Heat and Mass Transfer*, 45:2229–2242.

[10] Eijkel J.C.T., Berg A.V.D., (2005). Nanofluidics: what is it and what can we expect from it?, *Microfluid Nanofluid*, 1: 249–267.

[11] Kalweit M., Drikakis D., (2008). Coupling strategies for hybrid molecular–continuum simulation methods. Vol. 222 Part C: Journal of Mechanical Engineering Science, 222:797-806.

[12] Dussan E.B., (1979). Spreading of liquids on solid-surfaces-static and dynamic contact lines. *Annual Review of Fluid Mechanics*, 11: 371–400.

[13] Dussan E.B., Davis S.H., (1986). Stability in systems with moving contact lines. *Journal of Fluid Mechanics,* 173:115–130.

[14] Muradoglu M., Tasoglu S., (2009). Impact and Spreading of a Microdroplet on a Solid Wall. *7th International Conference on Nanochannels, Microchannels and Minichannels,* 1095-1106 Pohang, South Korea.

[15] Bussman M., Mostaghimi J., Chandra S., (1999). On a three-dimensional volume tracking model of droplet impact. *Physics of Fluids*, 11(6):1406-1417.

[16] Brackbill J.U., Kothe D.B., Zemach C., (1992). A continuum method for modeling surface tension", Journal of Computational Physics, 100:335-347.

[17] Blake T.D., Haynes J.M., (1969). Kinetics of liquid/liquid displacements. *Journal of Colloid Interface Science*, 30:421–423.

[18] Bayer I.S., Megaridis C.M., (2006). Contact angle dynamics in droplets impacting on flat surfaces with different wetting characteristics. *Journal of Fluid Mechanics*, 558:415–449

[19] Youngs D.L., (1984). An interface tracking method for a 3D Eulerian hydrodynamics code. *Technical Report 44/92/35*, AWRE.